Single-Lane 54-Gbit/s PAM-4/8 Signal Transmissions Using 10G-Class Directly Modulated Lasers Enabled by Low-Complexity Nonlinear Digital Equalization

Ahmed Galib Reza ⓘ, Marcos Troncoso-Costas ⓘ, *Graduate Student Member, IEEE*,
Colm Browning ⓘ, *Member, IEEE*, Francisco J. Diaz-Otero, and Liam P. Barry ⓘ, *Senior Member, IEEE*

Abstract—This work presents the use of a directly modulated laser (DML) in time- and wavelength division multiplexed passive optical networks (TWDM-PONs), in which an EDFA-based booster amplification and an SOA-based pre-amplification are utilized to improve the optical power budget. We experimentally demonstrate the C-band optically amplified data transmissions and compare the performance of the non-return-to-zero on-off keying (NRZ-OOK), four and eight-level pulse amplitude modulation (PAM-4/PAM-8) using a 10-G class DML. With optical amplification, the uplink and downlink power budgets of about 28 dB and 35 dB, respectively, are achieved for the PAM-4 54-Gbit/s signals at the hard-decision forward error correction (HD-FEC) limit of 3.8×10^{-3} after transmissions over a 25-km single-mode fiber link. To mitigate waveform distortions caused by the limited bandwidth, nonlinear dynamics, memory effects, and strong laser frequency chirp of the DML, especially during multi-level signal modulations, artificial neural network-based machine learning equalizers and low-complexity Volterra nonlinear equalizers are applied, which operate at the signal baud rate. The bit error ratio performance in conjunction with an enhanced power budget through the use of a low-complexity nonlinear equalizer can justify the validity of using a DML in the next-generation PONs.

Index Terms—Directly modulated laser, machine learning, nonlinearity, optical access networks, pulse amplitude modulation.

I. INTRODUCTION

IN RECENT years, the exponential evolution of newly developed bandwidth-hungry technologies such as high-definition (4K/8K) video streaming services, Internet of Things (IoT), Voice over IP (VoIP), video conferencing, and mobile front-haul and back-haul networks for the fifth- and the future sixth-generation (5G/6G) radio access network (RAN) to transport

large volumes of mixed data (mobile and fixed data), have been propelling the requirements for the development of higher data-rate optical access networks [1]. The passive optical network (PON) is well-established and can provide high-speed broadband services at a low capital and operational expenditures (CAPEX/OPEX). In 2015, the ITU Telecommunication Standardization Sector (ITU-T) released a new 40 Gbit/s-capable PON standard called the next-generation passive optical network 2 or NG-PON2 by integrating the time and wavelength-division multiplexing (TWDM) in the same PON [2]. However, NG-PON2 may not satisfy currently increasing bandwidth demand and capacity requirements, as the maximum achievable data rate per wavelength is limited to 10-Gbit/s. Very recently, the Institute of Electrical and Electronics Engineers (IEEE), ITU-T, and Full Services Access Network (FSAN) have made substantial efforts in the development of PON technology to meet the ever-increasing bandwidth demand. A new task force has been established by the IEEE to standardize 25, 50, and 100G Ethernet PON (EPON) by combining two or four wavelengths with the data rate of 25 or 50 Gb/s/λ [3].

Even though the coherent PON (CO-PON) can increase the data rate, receiver sensitivity, and spectral efficiency significantly [4]; it is not a near or medium-term solution for high-capacity access networks due to the current high cost of optical coherent transceivers. For example, a coherent PON system with a polarization diverse receiver will require two polarization beam splitters (PBSs), two 90º optical hybrids with four balanced photodetectors, four analog-to-digital converters (ADCs), and a local oscillator (LO) [5]. Therefore, it is important to design a 100-G class PON that will coexist in the same optical distribution network (ODN) and be compatible with the legacy PON. These are essential requirements for the evolution of PON technology from the operator's perspective, especially with a large number of ODNs [6]. Therefore, to date, all the suggested PON standards are based on intensity modulation and direct detection (IM/DD) technology due to its relatively simple architecture and low implementation cost [7], [8]. In this regard, the biggest challenges to increasing the data rate beyond 10-G are the bandwidth limitations of the electro-optic components, optical power budget, and the fiber's chromatic dispersion - especially in the 1550-nm (C-band) and 1600-nm band (L-band).

One possible way to overcome the issue of bandwidth limitation and to increase the dispersion tolerance of the PON system is to introduce higher-order modulation formats like electrical duobinary (EDB) [9] and PAM [8], [10], as they can increase the spectral efficiency of the transmission system and can be modulated using a low-cost DML, which is still the preferred option to realize PONs due to its simple architecture, low cost, high optical output power, and small footprint [11]. However, high nonlinear dynamics of the modulating laser, low modulation bandwidths, memory effects, and the interplay between the fiber chromatic dispersion and laser frequency chirp (both adiabatic and transient) can limit the performance of PAM-*M* systems for PON applications [12], [13].

To overcome the problem of nonlinear distortions and other impairments triggered by the optical/electrical components, the deployment of digital signal processing (DSP) technology [14], such as a combination of feed-forward and decision feedback equalizers (FFE/DFE) [15], nonlinear lookup table [16], Volterra nonlinear equalizer (VNLE) [17], [18], maximum likelihood sequence estimation (MLSE) [8], machine learning, e.g, artificial neural networks (ANNs) [13], [19], recurrent neural networks (RNNs) [20]–[23], and convolutional neural networks (CNNs) [7], [24] have become increasingly popular in recent years. Furthermore, the advances in forward error correction (FEC) can also satisfy the demand for high-capacity optical access networks with high loss budget requirements.

In this paper, we experimentally demonstrate single-wavelength 54-Gbit/s PAM-4 and PAM-8 transmissions with a 1540-nm DML over a 25-km single-mode fiber (SMF) link. By incorporating optical amplifiers, we report optical power budgets of about 28 dB and 35 dB for the PAM-4 signals in the uplink and downlink of a TWDM-PON, respectively. In this work, the power budgets of the PON system for the upstream and downstream transmissions are calculated by subtracting the minimum receiver sensitivity at the HD-FEC level bit error ratio (BER) performance from the signal launch power to the fiber and adding the gain of the optical amplifier. This paper extends upon previous works [25], [26], in which we aimed to find out the most suitable modulation format for the IM/DD PON systems with an improved power budget. Furthermore, we conduct a feasibility analysis of the VNLE and ANN-NLE that can alleviate the nonlinear distortions in the signal and derive the justification for using a DML in a high-speed PON scenario. Even though 50 Gbit/s or higher data rate transmissions have already been demonstrated for the access networks using 10-G modulators, the optical power budget requirement is still a challenging subject to study for such systems [7], [27]. It is worth mentioning that, in the downstream direction, we consider the use of an erbium-doped fiber amplifier (EDFA) at the optical line terminal (OLT) to boost multiple wavelengths in a WDM-PON scenario and a semiconductor optical amplifier (SOA) at a remote node (RN) to accommodate multiple splitters and optical network units (ONUs). In addition, an SOA can be used in the upstream direction of the system for pre-amplification at the OLT to enhance the optical power budget of the PON.

The rest of the paper is organized as follows. In Section II, the low-complexity Volterra nonlinear equalizer is presented; and
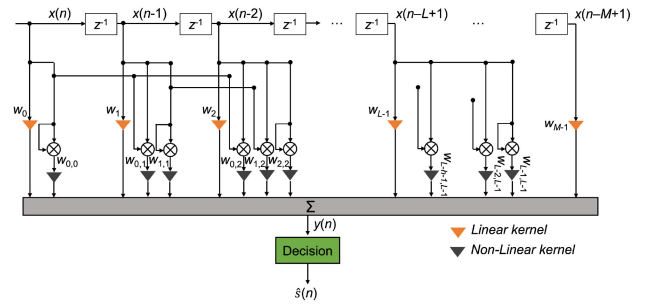

Fig. 1. Volterra nonlinear equalizer (VNLE) with *M* linear taps, and *L* nonlinear taps with *h* number of beating neighbors.

the ANN-based nonlinear equalizer is described in Section III. Section IV describes the DML-based TWDM-PON architecture, with the experimental setup being explained in Section V. Section VI presents the experimental results and gives an analysis of the performance of the TWDM-PON system after equalizations. Finally, in Section VII, we summarize our contributions and conclude the paper with some conclusive remarks.

II. VOLTERRA NONLINEAR EQUALIZER (VNLE)

Unlike a linear system, the nonlinear response of a DML with memory effects cannot be fully characterized based on the impulse response alone, as it can only tackle the linear inter-symbol interference (ISI) of the transmission system. Volterra series is one of the most popular mathematical models that can characterize a nonlinear system with memory effects [28].

It is well known that the Volterra series is a combination of a linear filter and polynomial expressions between the present and the past inputs. In this regard, the memory length of the Volterra series must be large enough for an accurate approximation of the nonlinear behavior of the system, resulting in an exponential rise of the nonlinear coefficients. This can impose a severe constraint on the application of the Volterra model due to a high implementation cost, processing complexity, and convergence issues. Therefore, it is imperative to decrease the memory length and the number of beating terms of the Volterra series for practical implementation in high-speed optical communication systems.

In this work, a low-complexity truncated second-order VNLE is considered [18], as shown in Fig. 1. Unlike the traditional VNLE, we have limited the number of cross-beating terms in the nonlinear part of the VNLE to reduce complexity, and also the numbers of taps for the linear and nonlinear parts of the VNLE are not equal. This stems from our finding that many nonlinear coefficients are not so effective in improving the system performance; especially the cross-beating terms that can become negligible if they contain signals received at long time delays and from distant neighbors. One alternative to reduce the complexity of the full-scale VNLE can be pruning, which discards the nonlinear kernels according to their weight values and requires retraining of the VNLE [29]; hence, it is not considered in this work. Table I shows the total number of nonlinear coefficients and complexity analysis for the second-order traditional and low-complexity VNLE.

TABLE I
THE TOTAL NUMBER OF NONLINEAR COEFFICIENTS FOR THE TRADITIONAL
AND TRUNCATED VNLE

Memory length (L)	Trad. VNLE	Truncated VNLE		
	No. of nonlinear coefficients	No. of beating terms (k)	No. of nonlinear coefficients	Complexity reduction (R)
10	55	3	27	50.91%
		5	40	27.27%
20	210	6	105	50.00%
		10	155	26.19%
30	465	9	234	49.68%
		15	345	25.81%
40	820	12	414	49.51%
		20	610	25.61%

The transfer function of a complex second order VNLE at time instant n can be expressed as:

$$y(n) = \sum_{m_1=0}^{M-1} w_{m_1}(n)x(n-m_1) + \sum_{m_1=0}^{L-1}$$

$$\times \sum_{m_2=m_1}^{min(m_1+h,L-1)} w_{m_1,m_2}(n)x(n-m_1)x(n-m_2) \quad (1)$$

where $x(n)$ denotes the input signal to the VNLE, $y(n)$ is the output of the nonlinear equalizer, $w_{m_1}(n)$ indicates the linear coefficients of the VNLE with the size of M, and $w_{m_1,m_2}(n)$ represents the nonlinear coefficients of the VNLE considering the memory length of L and the beating of as many as h neighboring signals.

In (1), the first-order inputs (linear terms) to the equalizer can only mitigate linear distortions, e.g., bandwidth limitation of the DML, and the second-order inputs (beating terms) are responsible for mitigating the dominant nonlinear distortions (second-order nonlinearity) of the system. Before equalizing the system output, the VNLE is required to find the linear and nonlinear tap weights, which can be obtained by using some adaptive algorithms, for example, least-mean square (LMS), recursive-least square (RLS), etc. In this work, the filter tap weights are adapted through a training sequence, in which the received distorted signals initially go through the linear and nonlinear sections of the equalizer to produce an estimate of the transmitted symbol. Subsequently, the estimated symbol is compared with the training symbol and the instantaneous error is used to update the weights of the VNLE.

III. ARTIFICIAL NEURAL NETWORK-BASED NONLINEAR EQUALIZER

In this paper, we present a multi-layer perceptron (MLP) network-based fully connected feed-forward neural network. It consists of three layers; the input layer, output layer, and hidden layer. The input layer receives the distorted input signal to be treated. The output layer produces the equalized system output. Several hidden layers can be placed between the input
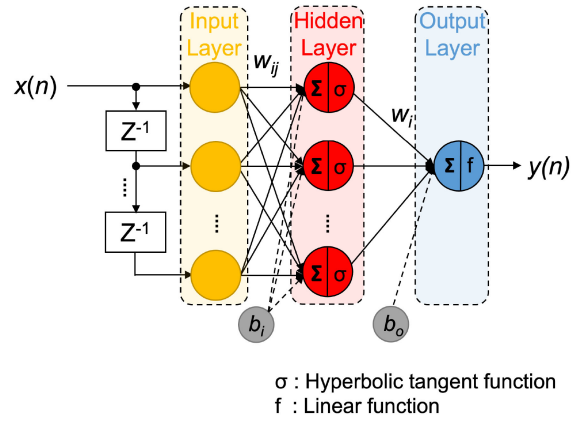

Fig. 2. Artificial neural network-based nonlinear equalizer (ANN-NLE) [13].

σ : Hyperbolic tangent function
f : Linear function

and output layers for data transformation. Fig. 2 illustrates the ANN-based nonlinear equalizer (ANN-NLE) to jointly mitigate the linear and nonlinear distortions of the signals induced by the DMLs. From the figure, we can see that the proposed ANN-NLE contains only a single hidden layer of computational nodes and only one output node in the output layer to reduce the implementation cost and processing complexity of the PON system. Currently, there is a great deal of interest in applying deep learning (two or more hidden layers in the network) to solve nonlinear problems, which might not be practical for the application of the IM/DD PON system due to increasing cost and computational complexity.

The ANN-NLE can accept a digital signal and produce an output at every discrete time instance. The output $y(n)$ of the ANN-NLE can be expressed using the following equation [13]:

$$y(n) = f\left(b_o + \sum_{i=1}^{r} w_i\sigma\left(b_i + \sum_{j=0}^{M-1} w_{ij}x(n-j)\right)\right). \quad (2)$$

In the above equation, M and r correspond to the number of nodes in the input and hidden layers, respectively. The input PAM signal to the ANN-NLE is denoted by the vector $x(.)$, w_{ij} defines the weight for the connection between the jth node of the input layer and the ith node at the hidden layer, w_i defines the weight from the ith node of the hidden layer to the output layer, and b_i as well as b_o respectively represent the biases for the ith node at the hidden layer and the output node at the output layer. The function $\sigma(\cdot)$ denotes the nonlinear activation function for the hidden layer, which is a hyperbolic tangent function in this case; while the function $f(\cdot)$ is a linear activation function for the output layer of the network.

Before equalization, the ANN-NLE enters a training phase based on the supervised learning techniques to adapt the connection weights and biases of the network. For the loss function, the mean squared error (MSE) function is utilized to calculate the error $e(n)$ between the equalizer output $y(n)$ and the transmitted signal $d(n)$ as

$$e(n) = \|d(n) - y(n)\|^2. \quad (3)$$

The errors in the network are calculated in the forward direction according to the equation given in (3). In each epoch, the
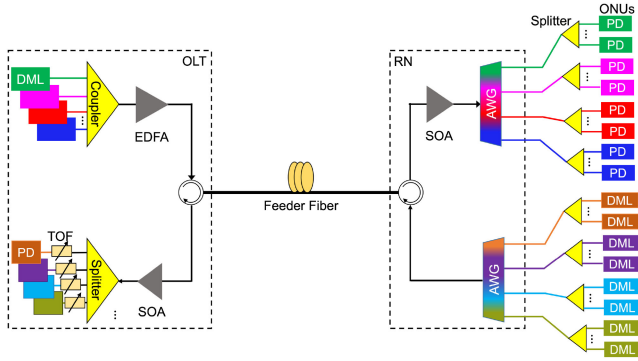
Fig. 3.   Conceptual architecture for the DML-based TWDM-PON system with an improved power budget using optical amplification.

Fig. 4.   The experimental setup for the DML-based single-lane 54-Gbit/s PAM transmission systems over 25-km SMF for the application of IM/DD-PONs. .

calculated errors are backpropagated in the network to adjust the connection weights and biases in a way that the error between the equalizer output and the actual signal can be minimized. To overcome the limitations of the traditional backpropagation algorithm such as local minima trap and slow speed of convergence, the Levenberg-Marquardt algorithm (LMA) is applied in this work. Using the LMA, the connection weights of the ANN-NLE can be updated using the following equation:

$$W_{k+1} = W_k - \left(J_k^T J_k + \mu I \right)^{-1} J_k e_k, \qquad (4)$$

where k is the iteration number, μ is a positive-valued scalar called the combination coefficient, I is a diagonal matrix in which the off-diagonal terms are zero, J is the Jacobian matrix, and e is the error vector of the neural network. The Jacobian matrix comprises the first-order partial derivatives of the error function with respect to the weights and biases, which can be obtained by applying a standard backpropagation technique without requiring calculating the complex Hessian matrix. In every iteration, the algorithm adjusts the connection weights and biases of the ANN-NLE until the desired error value is acquired or it has reached the maximum number of iterations. It is important to mention that when the training process is over, the data can flow only in the forward direction, from the input layer to the output layer.

IV. CONCEPTUAL NETWORK ARCHITECTURE

A conceptual network architecture for the IM-DD technology-based TWDM-PON is presented in Fig. 3, which is considered as a conceivable standard for the next-generation optical access network. In this design, a different set of wavelengths are assigned for the upstream and downstream transmissions.

In the downstream direction, a number DMLs based on distributed feedback (DFB) lasers operating on different wavelengths are used as the transmitters on the OLT side. To reduce cost, the outputs of the DMLs are combined by a passive coupler followed by EDFA amplification for loss budget improvement before being launched in the feeder fiber. After transmission, the signal is amplified at the remote node (RN) by an SOA before being demultiplexed by an arrayed waveguide grating (AWG). Even though the AWG offers a lower insertion loss, the SOA would be essential in this case to boost the power of the
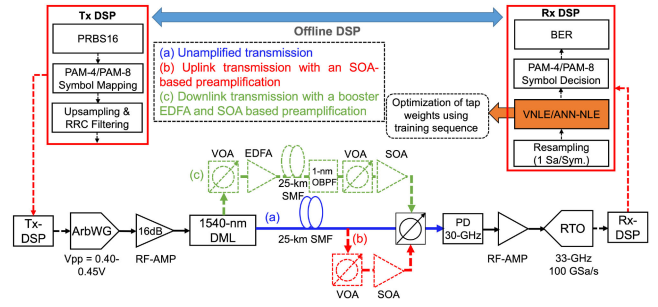
signals, which will eventually be distributed to multiple ONUs by employing a passive splitter. The insertion of a splitter will greatly increase the number of supported users in the network. We note here that an alternative architecture could involve the SOA placed after the AWG, with one SOA used to boost the signal on each wavelength.

In the upstream direction, a DML is used as the data source for the ONUs. In this scheme, since each wavelength is shared among many ONUs, the time-division multiplexing (TDM) protocol is essential for network operation. After applying the TDM to couple the data streams from ONUs with the same operating wavelength, the upstream signals from the distinctive groups of users, each with different wavelengths, are multiplexed at the RN by using an AWG. After fiber transmission through the feeder fiber, the upstream signals can initially be pre-amplified by an SOA to pre-compensate for the loss during wavelength demultiplexing by using a splitter followed by a tunable optical filter (TOF) before signal detection. At the OLT side of the network, the wavelength multiplexing/demultiplexing and optical amplification tasks are implemented as a single unit, which will enable it to coexist with the legacy PON system. For the upstream signaling, it is also feasible to consider an architecture in which the SOAs are employed at the RN to amplify the signals before or after the AWG, also to increase the system power budget. Despite the different possible architectures, the main goal of this work is to demonstrate that the ANN-based machine learning equalizers and low-complexity VNLE can indeed be used to enhance the performance of optically amplified 50-G PON systems using DMLs.

V. EXPERIMENTAL SETUP

In this paper, 54-Gbit/s NRZ-OOK, PAM-4, and PAM-8 signal transmissions are realized over a 25-km SMF in the C-band (1540-nm) using a 10-G class DML, which has a 3 dB bandwidth of around 15 GHz at the bias current of 55 mA.

The experimental setup for the IM/DD PON systems is illustrated in Fig. 4, in which the PAM signals are generated in MATLAB by using the pseudo-random bit sequences (PRBS) with a length of $2^{16} - 1$ and encoded using gray-coding with the help of the transmitter side offline DSP block. The generated PAM-4 and PAM-8 symbols are up-sampled to apply the root-raised cosine (RRC) pulse shaping with a roll-off factor of 0.3 to realize Nyquist pulse shaping and to match the fundamental

clock frequency of the arbitrary waveform generator (Keysight ArbWG M8196A) of 87.75 GSa/s and 90 GSa/s, respectively. The analog bandwidth of the Keysight ArbWG is 32-GHz, and the peak-to-peak voltage (Vpp) of the ArbWG outputs are optimized at 400mV and 450mV for the PAM-4 and PAM-8 signals, respectively. Generally, the system nonlinearity can be adjusted by properly setting the Vpp for each modulation format, and a higher Vpp is usually required for the signals with more levels. In the experiment, we amplify the output of the ArbWG by using a 16 dB gain RF amplifier with a bandwidth of 25-GHz. Next, the amplified RF signals are used to drive a commercial 1540-nm DML with the bias current of 70 mA and 55 mA for the PAM-4 and PAM-8 signals, respectively. Despite the lower extinction ratio achieved, the DML is biased at a high current for the PAM-4 signals to increase the DML bandwidth and to suppress the transient chirp, making the adiabatic chirp more dominant.

To emulate the various data flows included in the network architecture discussed in Section IV, three experimental scenarios are investigated in this paper as follows: (1) the NRZ-OOK, PAM-4, and PAM-8 modulated DML outputs are directly launched into a 25-km SMF link without any optical amplification, as presented in Fig. 4(a). The attenuation factor of the 25-km optical link is 0.2 dB/km. In this case, the system performance is compared against the various modulation techniques to verify the feasibility of using the multi-level signals in a short-haul transmission with a DML. (2) After 25-km transmission (upstream direction), the optical signal is attenuated to -7 dBm by a variable optical attenuator (VOA) to emulate the split loss in the OLT or RN side of the network and then boosted by an SOA with the gain of about 15 dB to improve the power budget, as presented in Fig. 4(b). (3) The DML output is attenuated to -4 dBm by a VOA before EDFA amplification (for downstream transmission) with 17.5 dB gain. After 25-km fiber transmissions, the PAM signals are attenuated to -7 dBm by a VOA followed by SOA amplification of the received signal to 8 dBm to boost the power budget of the network, as shown in Fig. 4(c).

After transmission, the PAM modulated optical signals are detected by using a 30-GHz photodetector with the responsivity of 0.7A/W at 1550-nm for optical-to-electrical conversion. To measure the sensitivity of the receiver, a VOA is placed before the photodetector for adjusting the received optical power (ROP). Next, the detected electrical signals are amplified with an RF amplifier before capturing with a 33-GHz bandwidth real-time oscilloscope (RTO) operating at 100 GSa/s (Tektronix DPO77002SX). To synchronize the reference clock between the ArbWG and RTO, the 10 MHz output reference clock of the RTO is used as the reference clock for the ArbWG. Afterward, the captured signal is sent to the receiver side offline DSP block for signal processing.

In the Rx-DSP block, after matched-filtering, we resample the output of the RTO at the signal baud rate of 27 and 18 GSa/s for the PAM-4 and PAM-8 signals, respectively, meaning that each digital PAM symbol consists of only 1 sample/symbol. Next, the digital PAM signals are sent to the nonlinear equalizers, as discussed in Sections II and III. After optimizing the DSP
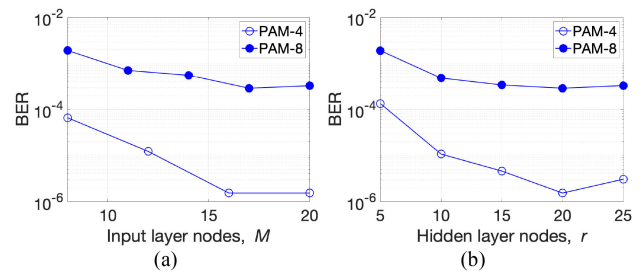

Fig. 5. (a) BER versus the number of nodes in the input layer. (b) BER versus the number of nodes in the hidden layer.
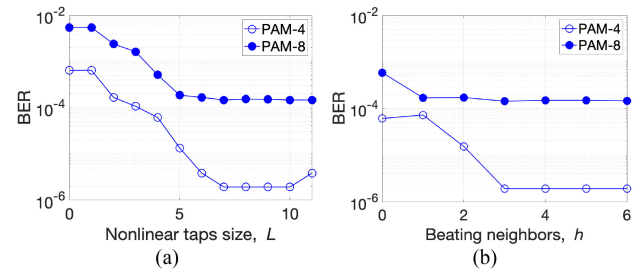

Fig. 6. (a) BER versus the nonlinear tap size L of the VNLE. (b) BER versus the number of beating neighbors h of the VNLE.

parameters and the tap weight adaptation process by employing a training sequence for the VNLE and ANN-NLE, the equalizers were placed to compensate for the linear and nonlinear distortions of the DML. After signal demodulation, the BER is calculated in MATLAB to investigate the performance of the transmission system.

VI. Experimental Results

First, we optimize the DSP parameters of the nonlinear equalizers in the case of 54-Gbit/s unamplified transmissions over a 25-km SMF link at -1 dBm ROP. Typically, this type of equalizer performs better with the receiver-side oversampling and a large number of filter taps, which might not be applicable for a high-speed optical access network due to the cost and implementation complexity. Furthermore, it is important to mention that throughout the experiments, the received signals are sampled at the signal baud rate, thus simplifying the system operation.

In Fig. 5(a) and (b), we plot the BER results versus the number of nodes in the input and hidden layers of the ANN-NLE, respectively. In Fig. 5(a), the number of nodes in the hidden layer was chosen to be 20, and in Fig. 5(b), we set the numbers of input layer nodes to 16 and 17 for the PAM-4 and PAM-8 signals, respectively, which is optimized in Fig. 5(a). As expected, the BER performance is improved as we increase the number of input layer nodes. Similar improvements in the performance are observed in Fig. 5(b), as we increase the number of hidden layer nodes. We can notice a slight degradation in the BER performance when the number of hidden layer nodes is increased to 25. The overfitting phenomenon of the machine learning technique could contribute to this performance degradation. Since the main objective of this plot is to reduce the complexity of the
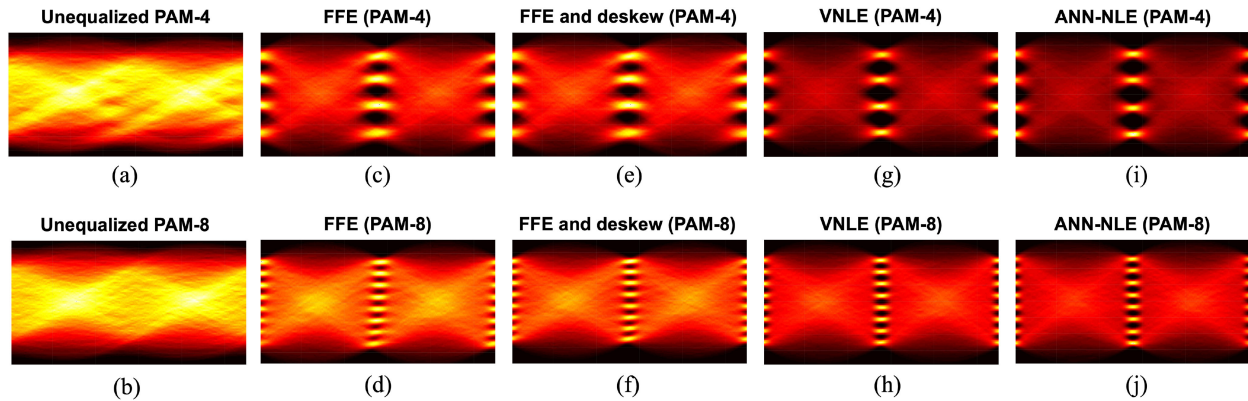
Fig. 7. Eye diagrams after 25-km unamplified signal transmissions. (a) Unequalized PAM-4 signals; (b) Unequalized PAM-8 signals; (c) PAM-4 signals after FFE; (d) PAM-8 signals after FFE; (e) PAM-4 signals after FFE and skew comensation; (f) PAM-8 signals after FFE and skew compensation; (g) PAM-4 signals after VNLE (h) PAM-8 signals after VNLE; (i) PAM-4 signals after ANN-NLE; and (j) PAM-8 signals after ANN-NLE.

ANN-NLE, we can optimize the number of input layer nodes at 16 and 17 for the PAM-4 and PAM-8 signals, respectively, and the number of hidden layer nodes at 20 for the rest of the experiments. By analyzing the implementation complexity of the ANN-NLE through counting the number of multiplications, we can conclude that the ANN-NLE needs to perform at least 340 and 360 multiplications to mitigate the nonlinear distortions of the PAM-4 and PAM -8 signals, respectively.

In Fig. 6, we optimize the nonlinear tap size L and the number of beating neighbors h of the VNLE used. In Fig. 6(a), $L = 0$ corresponds to the state of the traditional FFE. As anticipated, the VNLE performs better if we increase the number of nonlinear taps, and the best BER results can be attained with 7 nonlinear taps for both PAM-4 and PAM-8 signals. Further increase in the nonlinear taps does not show any noticeable difference in the performance. However, when L is increased to 11, overfitting may occur, and the performance degrades slightly. Next, in Fig. 6(b), we optimize the number of beating neighbors h, when $L = 7$. Here, $h = 0$ corresponds to the self-beating terms only, and $h = 6$ characterizes the case for the traditional second-order VNLE. From the figure, we can see that only the first three near neighbors of the VNLE have a major impact on the performance. The distant neighbors can be discarded since the complexity of the VNLE exponentially rise as we increase the number of beating neighbors, and no discrepancies in the BER performances are observed for the low-complexity truncated VNLE compared with the traditional VNLE. In the plot, the numbers of linear taps are fixed at 16 and 17 for the PAM-4 and PAM-8 signals, respectively, meaning the total number of multiplications needed to perform equalization are 60 and 61. Further analysis indicated an 80% reduction of the total multiplication cost for the truncated VNLE compared with the full-scale second-order VNLE.

In Fig. 7, we present the eye diagrams of the 54-Gbit/s multi-level PAM signals after 25-km unamplified transmissions at the ROP of -1 dBm. Complete eye closures are observed in the case of unequalized PAM-4 (Fig. 7(a)) and PAM-8 (Fig. 7(b)) signals. The equalized eye diagrams are presented in Fig. 7(c) and (d) using the FFE, which indicate poor eye-opening and nonlinear timing skew problem due to asymmetric rise and fall time of
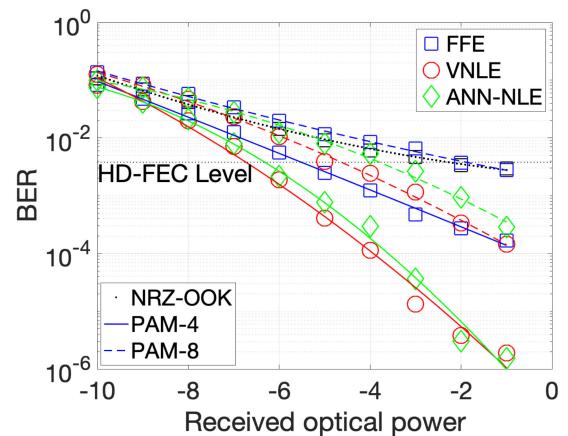

Fig. 8. BER versus ROP after 25-km unamplified transmission. The performances after FFE, VNLE, and ANN-NLE are presented by the square, circle, and diamond markers, respectively. Dotted line = NRZ-OOK; solid line = PAM-4; dashed line = PAM-8.

the DML and a sudden drop of the modulation bandwidth close to the threshold current. It is more obvious in the case of the PAM-8 signal (Fig. 7(d)) and a separate deskewing technique can be used in the receiver side DSP to improve performance (Fig. 7(e) and (f)). Unlike linear equalization, both VNLE and ANN-NLE (Fig. 7(g)–(j)) can equally mitigate the linear and nonlinear distortions of the PAM signals caused by the DMLs. We can see that the PAM-4 signals yield a larger eye-opening compared with the PAM-8 signals since the PAM-8 signals suffer more due to the nonlinear ISI penalty as the number of signal levels is higher.

Next, in Figs. 8 –10, we present the BER results after 25-km transmission for various transmission scenarios and ROPs. In the figures, the dotted, solid, and dashed lines respectively show the BER performances for the 54 Gbit/s NRZ-OOK, PAM-4, and PAM-8 signals. The assessments of system performance using three equalizers are presented in the plots (1) FFE (square markers), (2) VNLE (circle markers), and (3) ANN-NLE (diamond markers).

In Fig. 8, we plot the BERs with respect to the ROPs in the case of unamplified 25-km transmission. In the experiment,
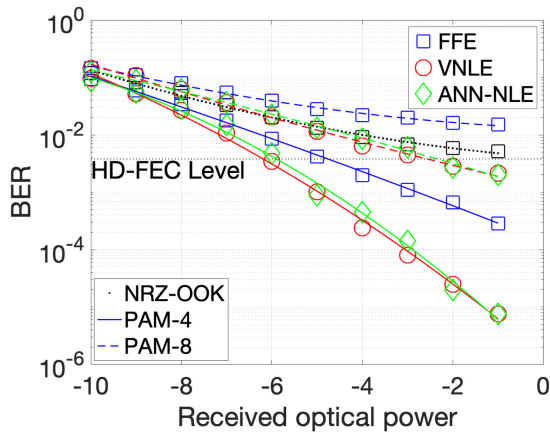
Fig. 9. BER versus ROP after 25-km optically amplified transmission using an SOA. The results after equalization with the FFE, VNLE, and ANN-NLE are shown by the square, circle, and diamond markers, respectively. Dotted line = NRZ-OOK; solid line = PAM-4; dashed line = PAM-8.
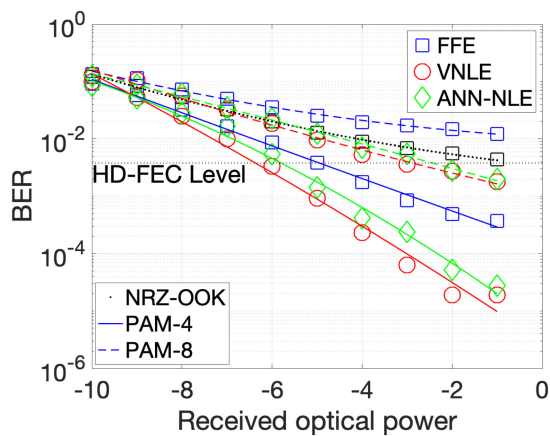

Fig. 10. BER versus ROP after 25-km optically amplified transmission using an EDFA and an SOA. The performances after the FFE, VNLE, and ANN-NLE equalizations are presented by the square, circle, and diamond markers, respectively. Dotted line = NRZ-OOK; solid line = PAM-4; dashed line = PAM-8. Dotted line = NRZ-OOK; solid line = PAM-4; dashed line = PAM-8.

the NRZ-OOK signal is equalized with a 16-tap FFE, and no significant improvement in the performance was observed when applying an ANN-NLE or VNLE, as the effects of the nonlinear penalties such as memory effects, asymmetric rise and fall time, and nonlinear dynamics of the DMLs are less of an issue for the two-level NRZ-OOK signal. For comparisons, we also plot the BER performances of the PAM-4 and PAM-8 signals after FFE, VNLE, and ANN-NLE while maintaining the same data rate of 54-Gbit/s. Note that for the FFE, we utilized a separate skew compensation block at the receiver DSP and observed a marked improvement in the performance. However, such deskewing techniques are not essential for the nonlinear equalizers, as presented in Fig. 7. Among the three modulation formats, the PAM-4 produces the best, and the NRZ-OOK generates the worst BER performances. We found that the 16-tap FFE can mitigate the issue of bandwidth limitation of the DML for the NRZ-OOK signal to some extent, as the HD-FEC level BER performances can be achieved at the ROP of -2 dBm, whereas the unequalized NRZ-OOK signal produces the BERs of above 10^{-1}

for any ROPs. This is primarily due to the fact that the modulation bandwidth of the 10-G class DML is considerably low to achieve 54-Gbit/s transmissions. Additionally, the NRZ-OOK experiences the maximum dispersion penalty as the spectral efficiency of the NRZ-OOK signal is the lowest. When using the nonlinear equalizers, we can see that the PAM-4 signals provide more than 2 dB better sensitivity compared with the PAM-8 signals. Furthermore, the performances of PAM-8 signal transmissions with the FFE are slightly worse than that of the NRZ-OOK. It indicates that even though the bandwidth limitation of a DML is an important problem to address, the issues of the nonlinear response of the DML, memory effects, and laser frequency chirp are even more serious; thus, a nonlinear equalizer is critically required for multi-level signal transmission with a DML to achieve a reasonable performance. Furthermore, we can see that the low-complexity VNLE can achieve a gain of about 0.5 dB compared with the ANN-NLE in the case of PAM-4 signal at a pre-FEC BER of 3.8×10^{-3}. The performance gap for the VNLE is further broadened in the case of the PAM-8 signal compared with the ANN-NLE.

In Fig. 9, we plot the BER results for optically amplified transmission using an SOA. From the BER curves, we can see that the FFE performed the worst among the three equalizers, and the NRZ-OOK cannot reach the HD-FEC level BER performance under any ROPs. For the PAM-4 signals, there is less than 0.5 dB supplementary penalty at the HD-FEC level due to the inclusion of an SOA in the experiment compared with the unamplified transmission, when using the ANN-NLE for signal equalization. On the contrary, the sensitivity penalty of about 2 dB is observed for the PAM-8 signal. We report that similar BER performances can be maintained for the PAM-4 signals with an improved power budget of 28.2 dB at a pre-FEC BER of 3.8×10^{-3} compared with the unamplified transmission scenario.

In Fig. 10, we plot the BER results as a function of the ROP for optically amplified transmissions using an EDFA at the OLT-Tx and an SOA to increase the power budget and the potential number of users in the downstream transmission. From the PAM-4 BER curves, we can see no significant additional nonlinear penalties, where the ANN-NLE is used, due to the insertion of an EDFA and high-power fiber propagation. For the VNLE, a small power penalty of 0.2 dB is observed. We report that similar BER performances can be maintained with an improved power budget of about 35 dB at a pre-FEC BER of 3.8×10^{-3} utilizing nonlinear equalizers.

Finally, in Fig. 11(a) and (b), we plot the convergence curves of the VNLE and ANN-NLE after 25-km unamplified PAM-4 signal transmissions, respectively. From the VNLE convergence curve, we can observe that the instantaneous MSE can vary between the range of 10^0 and 10^{-2}. However, after convergence, the average MSE will fall in the range of 10^{-1}. To prevent overfitting, we can allow a maximum of 500 iterations in this case before stopping the training process. For the VNLE, the linear and nonlinear tap coefficients are calculated using the RLS and LMS algorithms, respectively. For the ANN-NLE, convergence can be achieved with less than 50 epochs. To train the ANN-NLE, 4096 PAM-4 symbols were utilized in the experiment. From the BER results, we found that both techniques can produce
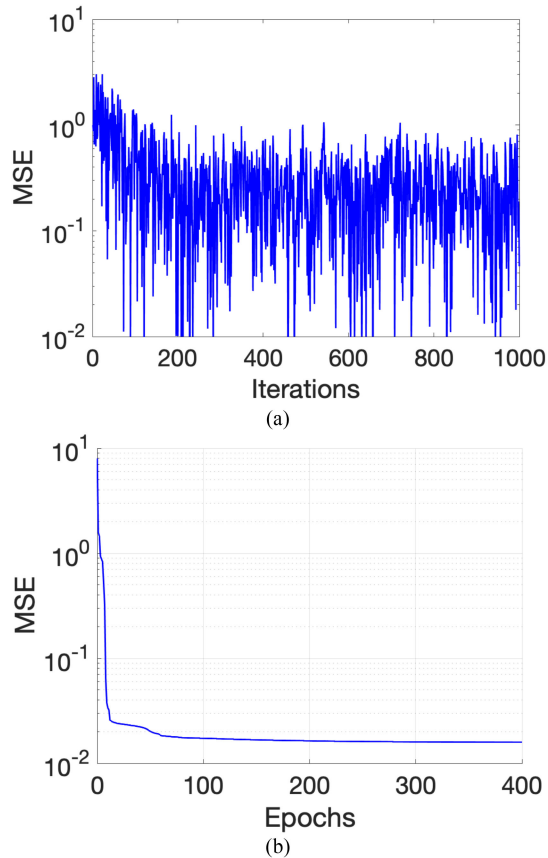
Fig. 11. Convergence curve in the context of mean squared error (MSE). (a) VNLE. (b) ANN-NLE.

comparable performances. Even though the experiments were only conducted under the traditional continuous-mode operation, the ANN-NLE and VNLE can be suitable for the upstream burst-mode operations in the TWDM-PON architecture, as the equalizers can achieve reasonably fast convergence (about 19 ns for the VNLE, and 7 μs for the ANN-NLE, calculated based on the number of training symbols, epochs, and iterations required to achieve a steady-state performance) and the nonlinearities of the systems are usually static and do not vary much over time.

VII. CONCLUSION

We have demonstrated single-lane 54-Gbit/s transmissions over a 25-km SMF with a 10-G class DML. The conceptual TWDM-PON design attained a 35 dB power budget in the downlink and a 28 dB power budget in the uplink by utilizing optical amplification and nonlinear digital equalizations. Even though the link budgets are different for the uplink and downlink, the experimental results in the downstream direction indicate that careful placement of an SOA at the RN in the uplink could potentially mitigate the issue without any noticeable performance degradation. Furthermore, in the Rx-side DSP, all the equalizers are operating at the rate of 1 Sample/Symbol, which simplifies the processing and makes the system implementation more practical. Even though the experiment is conducted for a single channel, the proposed scheme can be suitable for

the TWDM-PON transmission systems, considering the power budget achieved in the experiments. In this paper, we found that the PAM-4 modulation format is an ideal choice for the IM/DD PON, as it can significantly boost the receiver sensitivity with nonlinear digital equalization compared with the NRZ and PAM-8 signals, considering both unamplified and amplified transmission scenarios.

We found that, compared to the ANN-NLE, the VNLE requires a lower number of multiplication operations, it can achieve faster convergence and slightly better BER performances. However, the ANN-NLE holds the distinctive advantage that it can be easily implemented with a lookup table, making it fast, efficient, and a feasible choice to implement with Reconfigurable Field-Programmable Gate Arrays (FPGAs). On the contrary, the VNLE requires a polynomial-based multiplication between two unknown samples, which significantly increases the hardware resource requirements, processing delays, and power consumption for hardware implementation of the VNLE.

Overall, the implementation of the DSP and networking approaches explored in this work can provide a pathway for the continued deployment of simple and cost-effective direct modulation-based optical access networks capable of meeting the next-generation speeds and power budget constraints.

REFERENCES

[1] I. Tomkos, L. Kazovsky, and K. I. Kitayama, "Next-generation optical access networks: Dynamic bandwidth allocation, resource use optimization, and QoS improvements," *IEEE Netw.*, vol. 26, no. 2, pp. 4–6, Mar./Apr. 2012.

[2] "40 gigabit-capable passive optical networks (NG-PON2): General requirements," ITU-T recommendation G.989.1, 2015. [Online]. Available: https://www.itu.int/rec/T-REC-G.989.1/en

[3] "IEEE P802.3ca 100G-EPON task force, Physical layer specifications and management parameters for 25 Gb/s, 50 Gb/s, and 100 Gb/s passive optical networks," 2015. [Online]. Available: http://www.ieee802.org/3/ca/

[4] Z. Li, F. Yin, X. Huang, Z. Ma, Y. Song, and L. Yi, "Demonstration of a 50G-PON with a 45-dB power budget using an IQ-interleaved coherent detection scheme," *Opt. Exp.*, vol. 29, no. 20, pp. 32523–32534, 2021.

[5] D. Lavery, S. Erkılınç, P. Bayvel, and R. I. Killey, "Recent progress and outlook for coherent PON," in *Proc. Opt. Fiber Commun. Conf.*, San Diego, CA, USA: Mar. 2018, pp. 1–3.

[6] C. Knittle, "IEEE 50 Gb/s EPON (50G-EPON)," in *Proc. Opt. Fiber Commun. Conf.*, San Diego, CA, USA: Mar. 2020, pp. 1–8.

[7] P. Li, L. Yi, L. Xue, and W. Hu, "56 Gbps IM/DD PON based on 10G-class optical devices with 29 dB loss budget enabled by machine learning," in *Proc. Opt. Fiber Commun. Conf.*, San Diego, CA, USA: Mar. 2018, pp. 1–3.

[8] Q. Guo *et al.*, "Experiment demonstration of IM-DD based 50-Gbps PAM4 TDM-PON downstream scheme enabled by transmitter pre-emphasis and MLSE," in *Proc. Opto-Electron. Commun. Conf.*, Jeju, Korea, Jul. 2018, pp. 1–2, Paper 5A2-3.

[9] B. Moeneclaey *et al.*, "40-Gb/s TDM-PON downstream link with low-cost EML transmitter and APD-based electrical duobinary receiver," *J. Lightw. Technol.*, vol. 35, no. 4, pp. 1083–1089, 2017.

[10] A. G. Reza and J. K. Rhee, "30-Gb/s PAM-8 transmission with directly-modulated laser using machine learning equalizer," in *Proc. Asia Commun. Photon. Conf.*, Hangzhou, China, Oct. 2018, pp. 1–3, Paper Su3C.5.

[11] M. Kim, S. H. Bae, H. Kim, and Y. C. Chung, "Transmission of 56-Gb/s PAM-4 signal over 20 km of SSMF using a 1.55-μm directly-modulated laser," in *Proc. Opt. Fiber Commun. Conf.*, Los Angeles, CA, USA: Mar. 2017, pp. 1–3, Paper Tu2D.6.

[12] K. Zhang, Q. Zhuge, H. Xin, W. Hu, and D. V. Plant, "Performance comparison of DML, EML and MZM in dispersion-unmanaged short reach transmissions with digital signal processing," *Opt. Exp.*, vol. 26, no. 26, pp. 34288–34304, 2018.

[13] A. G. Reza and J. K. Rhee, "Nonlinear equalizer based on neural networks for PAM-4 signal transmission using DML," *IEEE Photon. Technol. Lett.*, vol. 30, no. 15, pp. 1416–1419, Aug. 2018.

[14] R. I. Killey, "Towards 50G/100G passive optical networks with digital equalisation and coherent detection," in *Proc. Conf. Lasers Electro-Opt. Eur. Eur. Quantum Electron. Conf.*, Munich, Germany Jun. 2021, pp. 1–1, Paper ci_2_1.

[15] Z. Li *et al.*, "Investigation on the equalization techniques for 10G-class optics enabled 25G-EPON," *Opt. Exp.*, vol. 25, no. 14, pp. 16228–16234, 2017.

[16] J. Zhang, J. Yu, and H. Chien, "EML-based IM/DD 400G (4×112.5-Gbit/s) PAM-4 over 80 km SSMF based on linear pre-equalization and nonlinear LUT pre-distortion for inter-DCI applications," in *Proc. Opt. Fiber Commun. Conf. Expo.*, Los Angeles, CA, USA: Mar. 2017, pp. 1–3, Paper W4I.4.

[17] A. G. Reza and J. K. K. Rhee, "Blind nonlinearity mitigation of 10G DMLs using sparse Volterra equalizer in IM/DD PAM-4 transmission systems," *Opt. Fiber Technol.*, vol. 59, 2020, Art. no. 102322.

[18] N.-P. Diamantopoulos *et al.*, "On the complexity reduction of the second-order Volterra nonlinear equalizer for IM/DD systems," *J. Lightw. Technol.*, vol. 37, no. 4, pp. 1214–1224, 2019.

[19] Z. Xu, S. Dong, J. H. Manton, and W. Shieh, "Low-complexity multi-task learning aided neural networks for equalization in short-reach optical interconnects," *J. Lightw. Technol.*, vol. 40, no. 1, pp. 45–54, 2022.

[20] X. Huang, D. Zhang, X. Hu, C. Ye, and K. Zhang, "Recurrent neural network based equalizer with embedded parallelization for 100 Gbps/λ PON," in *Proc. Opt. Fiber Commun. Conf.*, San Francisco, CA, USA, Jun. 2021, pp. 1–3.

[21] Z. Xu, C. Sun, T. Ji, H. Ji, and W. Shieh, "Cascade recurrent neural network enabled 100-Gb/s PAM4 short-reach optical link based on DML," in *Proc. Opt. Fiber Commun. Conf. Expo.*, San Diego, CA, USA, Mar. 2020, pp. 1–3.

[22] B. Karanov, D. Lavery, P. Bayvel, and L. Schmalen, "End-to-end optimized transmission over dispersive intensity-modulated channels using bidirectional recurrent neural networks," *Opt. Exp.*, vol. 27, no. 14, pp. 19650–19663, 2019.

[23] C. Ye, D. Zhang, X. Hu, X. Huang, H. Feng, and K. Zhang, "Recurrent neural network (RNN) based end-to-end nonlinear management for symmetrical 50 Gbps NRZ PON with 29 dB+ loss budget," in *Proc. Eur. Conf. Opt. Commun.*, Rome, Italy, Sep. 2018, pp. 1–3.

[24] C. -Y. Chuang *et al.*, "Convolutional neural network based nonlinear classifier for 112-Gbps high speed optical link," in *Proc. Opt. Fiber Commun. Conf.*, San Diego, CA, USA, Mar. 2018, pp. W2A–W43.

[25] A. G. Reza, M. T. Costas, L. Barry, and C. Browning, "54-Gbit/s PAM-8 transmission in next-generation passive optical networks using directly modulated lasers with machine learning techniques," in *Proc. 13th Int. Congr. Ultra Mod. Telecommun. Control Syst. Workshops*, Brno, Czech Republic, Oct. 2021, pp. 278–281.

[26] A. G. Reza, M. T. Costas, C. Browning, and L. Barry, "High-speed PAM-4 signal transmissions with directly modulated lasers for the next-generation passive optical networks," in *Proc. 12th Int. Conf. Inf. Commun. Technol. Converg.*, Jeju Island, Korea, Oct. 2021, pp. 747–749.

[27] X. Miao, M. Bi, J. Yu, L. Li, and W. Hu, "SVM-modified-FFE enabled chirp management for 10G DML-based 50Gb/s/λ PAM4 IM-DD PON," in *Proc. Opt. Fiber Commun. Conf.*, San Diego, CA, USA: Mar. 2019, pp. M2B–M25.

[28] V. Volterra, "Sopra le funzioni che dipendono de altre funzioni," *Tipografia della R. Accademia dei Lincei*, vol. 3, pp. 97–105, 1887.

[29] G. S. Yadav, C.-Y. Chuang, K.-M. Feng, J.-H. Yan, J. Chen, and Y.-K. Chen, "Reducing computation complexity by using elastic net regularization based pruned Volterra equalization in a 80 Gbps PAM-4 signal for inter-data center interconnects," *Opt. Exp.*, vol. 28, no. 26, pp. 38539–38552, 2020.